Polymer Journal (2010) 42, 58–65

www.nature.com/pj

ORIGINAL ARTICLE

Poly(methyl methacrylate) (PMMA)-based hybrid materials with reactive zirconium oxide nanocrystals

Takeshi Otsuka,[1,2] and Yoshiki Chujo[2]

Highly transparent and homogeneous hybrids containing a single nano-sized inorganic oxide domain were synthesized from poly(methyl methacrylate) (PMMA) and aqueous dispersed zirconium oxide nanocrystals (ZrO_2-NCs) in the presence of a coupling agent, 3-(methacryloxy)propyl-trimethoxysilane (MPTS), which was grafted onto the surface of ZrO_2-NCs by zirconium hydroxide (Zr-OH) surface groups. The surface-functionalized ZrO_2-NCs were used as macromonomers in the process of grafting from polymerization of methyl methacrylate (MMA). The densities of surface Zr-OH groups and MPTS surface modifications were determined using thermogravimetric analysis. Fourier transform infrared analysis indicated successful bonding between organic and inorganic moieties. The morphology of the obtained hybrid films was investigated by scanning electron microscopy and tapping-mode atomic force microscopy. Hybrid films possess interesting thermal stability and optical transparency characteristics because of the uniform incorporation of networks between organic polymer chains and inorganic nanocrystals.
Polymer Journal (2010) **42,** 58–65; doi:10.1038/pj.2009.309

Keywords: macromonomer; nanocrystal; organic–inorganic hybrid; PMMA; transparency; ZrO_2

INTRODUCTION

Organic–inorganic hybrid nanocomposite materials have been studied in recent years, with the expectation that nanocomposite materials will serve as an important and evolutionary means of achieving properties that cannot be realized with single materials.[1–3] Composite materials with nanoscale domains show unique chemical and physical properties that are different from composites with microscale domains.[4–6] Organic–inorganic hybrids, in which organic polymers are dispersed in the inorganic phase at the nanometer or molecular level, have been widely investigated because of the unique properties that result from nanometer-length scales, such as high gas-barrier properties and excellent solvent resistance, flame resistance and high transparency. Optical transparency is the most important characteristic of these hybrids and it arises because dispersion of material in the matrix is in the order of tens of nanometers, far less than the wavelength of visible and ultraviolet light. As a result, light is not lost due to scattering.[7]

The most simple and convenient idea for construction of transparent and homogeneous hybrid materials is to increase the affinity between organic polymer and inorganic phases. Organic–inorganic hybrid materials are generally prepared by incorporating covalent bonds[8–13] or by physical interactions[14–21] to improve the compatibility between organic and inorganic phases.

Poly(methyl methacrylate) (PMMA) is an excellent material because of its potential application in optical fibers, optical disks and lenses. When PMMA is combined with inorganic materials such as SiO_2, TiO_2 or zirconium oxide (ZrO_2) at the nanometer level, the resulting hybrid materials have high strength and thermal stability.[22,23] In studies of PMMA/inorganic oxide materials, the inorganic network in hybrid materials is generally prepared from metal alkoxides[24–26] or colloidal inorganic nanoparticles.[27–30] There are many reports that base the preparation of PMMA/SiO_2 hybrid materials on unfunctionalized and trialkoxysilyl-functionalized acrylic polymers using an *in situ* sol-gel process in the presence of tetraethoxysilane (TEOS) or $Ti(OBu)_4$. In this case, the polymerization of monomers and the hydrolysis and condensation of TEOS occur simultaneously.[24–26,31–33] On the other hand, the colloidal silica approach provides the advantage of precise control on size distribution in hybrid materials. Colloidal silica with a particle size of <100 nm is required to avoid light diffraction. Large particles with a high refractive index, such as TiO_2 or ZrO_2, result in optical scattering and material opacity, thus limiting the optical applications of these hybrid materials. Small particles with a diameter <10 nm can avoid Rayleigh scattering and be incorporated into a polymer matrix while preserving optical transparency. There are a few reports of the synthesis of crystalline ZrO_2 with an average particle size below 5 nm.[34,35] Furthermore, in these reports, ZrO_2 dispersions are colored, which restricts their application potential. Recently, because of improvements in manufacturing processes, we were able to obtain nonaggregated ZrO_2 nanocrystals (3 nm) in an aqueous solution.[36] This ZrO_2 nanocrystal aqueous sol is colorless and suitable for use in the preparation of organic polymer and ZrO_2 hybrid materials.[37]

Herein, we report the synthesis of PMMA/ZrO_2 nanocrystal (ZrO_2-NC) hybrids with a coupling agent, 3-(methacryloxy)propyl-

[1]Sumitomo Osaka Cement Co., Ltd, Chiba, Japan; [2]Department of Polymer Chemistry, Graduate School of Engineering, Kyoto University, Kyoto, Japan
Correspondence: Professor Y Chujo, Department of Polymer Chemistry, Graduate School of Engineering, Kyoto University, Katsura, Nishikyo-ku, Kyoto 615-8510, Japan.
E-mail: chujo@chujo.synchem.kyoto-u.ac.jp
Received 3 July 2009; revised 10 September 2009; accepted 13 September 2009

trimethoxysilane (MPTS), grafted onto the surface of ZrO_2-NCs by zirconium hydroxide groups. The ZrO_2-NCs functionalized with MPTS were used as macromonomers in the polymerization of methyl methacrylate (MMA). Turner *et al.*[38,39] studied the characterization of MPTS grafted onto the surface of ZrO_2 particles and found that organic silane molecules (MPTS) covalently bond to the surface of ZrO_2 particles. However, in that study, the particles in the ZrO_2 powder were relatively large, with an average diameter of ~30 nm, which is too large to be suitable for optical applications because of Rayleigh scattering.

In this paper, we modify ZrO_2-NCs with MPTS for the polymerization of MMA, allowing for the covalent bonding of PMMA to ZrO_2 particles and ultimately the fabrication of transparent PMMA/ZrO_2-NC hybrid materials. PMMA/ZrO_2-NC hybrids, with hybrid domains in the order of a nanometer in size, show excellent transparency compared with that of PMMA/ZrO_2-NC blend composites with larger domain sizes. We also investigate the reinforcement of PMMA with ZrO_2 nanocrystals, which have excellent thermal stability. We show the potential of the transparent and homogeneous PMMA/ZrO_2 hybrids fabricated with inorganic nanocrystals for use in optical functional materials and coatings.

EXPERIMENTAL PROCEDURE

Materials

Methyl methacrylate monomer was purified by distillation under a vacuum. Azobisisobutyronitrile was recrystallized from ethanol at 35 °C. MPTS was purchased from Shin-Etsu Chemical (Tokyo, Japan). ZrO_2-NC aqueous sols, containing 10.0 wt% ZrO_2 with chloride anion (pH 2.0) and acetate anion (pH 1.7), were obtained from Sumitomo Osaka Cement (Chiba, Japan). ZrO_2-NCs have a primary particle size of 3 nm, with a particle size distribution in aqueous sols of 4.8 ± 1.2 nm.[37] Methanol was dried and distilled from magnesium methoxide and stored under nitrogen. 2-Ethoxyethanol was distilled under reduced pressure and stored under nitrogen. The other reagents were used without further purification.

Measurements

Fourier transform infrared (FT-IR) spectra were obtained using a Perkin Elmer 2000 infrared spectrometer (PerkinElmer Inc., Waltham, MA, USA) using the KBr pellet method. Scanning electron microscopy (SEM) measurements were determined using a JSM-5600B system (JEOL, Tokyo, Japan). Surface images were measured using tapping-mode atomic force microscopy (TM-AFM) (SPA 400, SEIKO Instruments, Chiba, Japan) operating at room temperature. Height and phase images were recorded simultaneously using nanoprobe cantilevers (SI-DF20, SEIKO Instruments). Transmission electron microscopy (TEM) was performed with a JEM-100SX microscope (JEOL) at 100 kV. Specimens for sectional analysis were prepared using a focused ion beam (SMI2050, SEIKO Instruments). Differential scanning calorimetry thermograms were obtained with a DSC200 (SEIKO Instruments) at a heating rate of 10 °C min^{-1} under nitrogen atmosphere. Thermogravimetric analysis (TGA) was carried out using TGA/DTA6200 (SEIKO Instruments) at a heating rate of 10 °C min^{-1} in air. Ultraviolet-visible transmission spectra were measured with a model MPS-2000 multipurpose spectrometer (Shimadzu, Kyoto, Japan). Refractive index was determined by a model 2010 prism coupler (Metricon Corporation, Pennington, NJ, USA).

Preparation of MPTS-modified ZrO_2-NCs as macromonomers

The preparation of MPTS-modified ZrO_2-NCs is shown in Scheme 1(a). ZrO_2-NC aqueous sol was gradually replaced by methanol using a rotary evaporator.

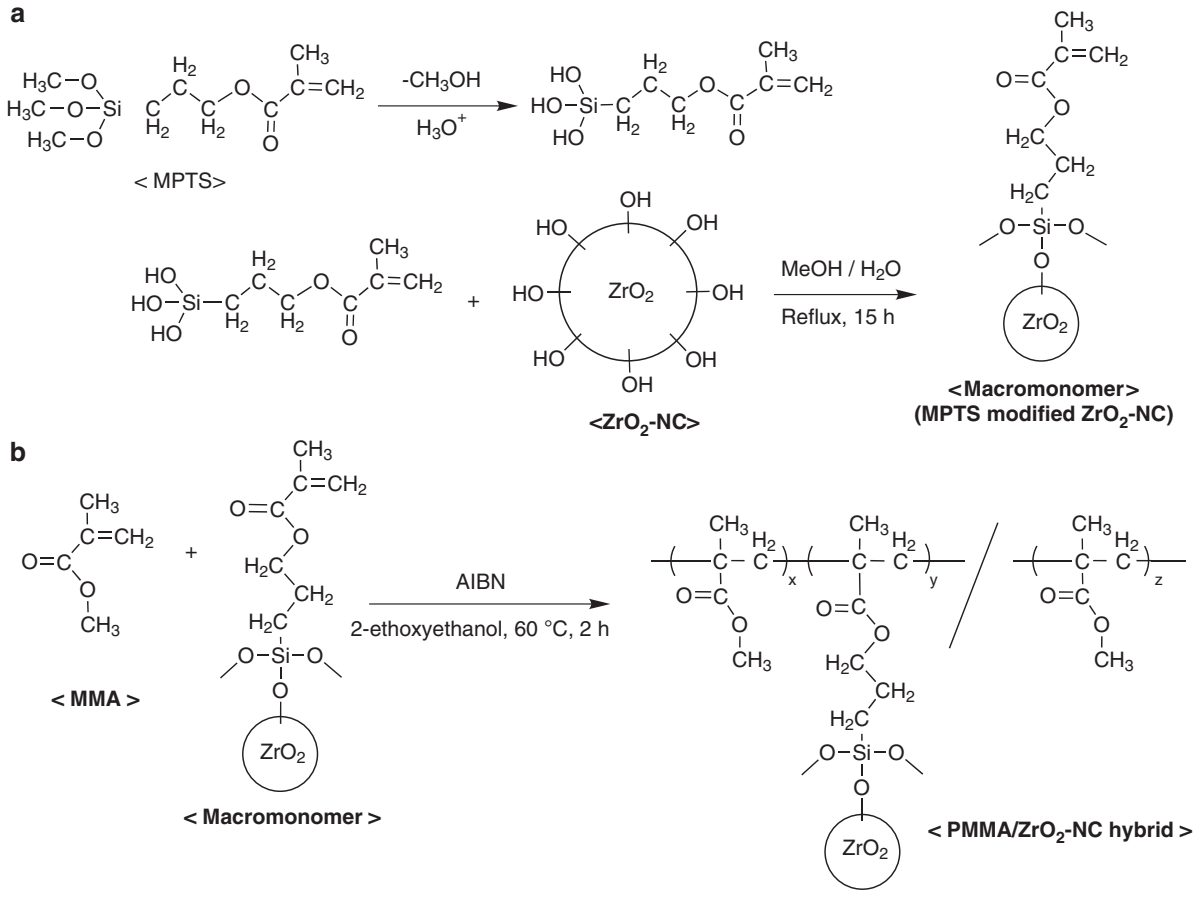

Scheme 1 Reaction route for preparing (**a**) 3-(methacryloxy)propyl-trimethoxysilane (MPTS)-modified zirconium oxide nanocrystals (ZrO_2-NCs) as macromonomers and (**b**) poly(methyl methacrylate) (PMMA)/ZrO_2-NC hybrid materials.

Table 1 Synthesis of PMMA/ZrO_2-NC hybrids

Run	MMA/MPTS-ZrO_2 ratio (mol/mol)	MMA (ml)	MPTS-modified ZrO_2-NC[a] (mg)	AIBN[b] (mg)	2-Ethoxyethanol (ml)	Sol appearance after polymerization	Film appearance
1	1/1	0.055	250	5.06	10	Precipitate	Crumble
2	5/1	0.274	250	15.20	10	Translucent	Cracked
3	10/1	0.547	250	27.85	10	Translucent	Transparent
4	25/1	1.369	250	65.84	10	Transparent	Transparent
5[c]	1/0	1.507	0	69.69	10	Transparent	Transparent

Abbreviations: AIBN, azobisisobutyronitrile; MMA, methyl methacrylate; MPTS, 3-(methacryloxy)propyl-trimethoxysilane; PMMA, poly(methyl methacrylate); ZrO_2-NCs, zirconium oxide nanocrystals.
[a]MPTS-modified ZrO_2-NC (Table 3, M-3) was used.
[b]AIBN/(MMA+MPTS)=3.0 mol%.
[c]8.35 wt% of PMMA solution was obtained.

Table 2 Preparation of PMMA/ZrO_2-NC blend composites[a]

Run	PMMA solution[b] (g)	Surface-modified ZrO_2-NC (mg)	Surface modifier	Sol appearance	Film appearance
6	1.00	100	Acetate anion[c]	Transparent	Turbid
7	0.70	100	MPTS[d]	Transparent	Translucent

Abbreviations: MPTS, 3-(methacryloxy)propyl-trimethoxysilane; PMMA, poly(methyl methacrylate); ZrO_2-NCs, zirconium oxide nanocrystals.
[a]Compositions of PMMA and ZrO_2-NCs were fixed about 35 wt% ceramic yields.
[b]PMMA solution (Table 1, Run 5) was used.
[c]The ZrO_2-NC powder, which was obtained from evaporation of aqueous sol with acetate anion (pH 1.7), was used. The amount of surface attached acetate anion was 19.7 wt% by thermogravimetric analysis.
[d]MPTS-modified ZrO_2-NCs (Table 3, M-3) was used.

The transparent methanol/water solution with 2.5 wt% ZrO_2-NC was cooled in an ice-cold water bath with vigorous stirring under nitrogen atmosphere. MPTS was added dropwise to the ZrO_2-NC solution using a syringe inserted through a septum and the reaction mixture was stirred for 30 min. The feed mole ratios of MPTS to ZrO_2 were 0.25–0.50 to 1.0. The mixture was then refluxed and stirred vigorously for 15 h, at which point the solution seemed slightly smoky. The resulting solution was concentrated and the residue was poured into water to precipitate the reactant. The MPTS-modified ZrO_2-NCs precipitate was filtered, carefully washed with a water/methanol solution and dried in vacuum at 30 °C.

Synthesis of PMMA/ZrO_2-NC hybrid sols

The polymerization of MMA with macromonomers is shown in Scheme 1(b). Under a nitrogen atmosphere, the obtained MPTS-modified ZrO_2-NCs (serving as a macromonomer), MMA monomer and azobisisobutyronitrile were dissolved in 2-ethoxyethanol at the compositions shown in Table 1 and stirred for 1 h at room temperature. The resulting solution was heated to begin the radical polymerization reaction. The reaction temperature was maintained at 60 °C and the solution was stirred under a nitrogen flow for 2 h to obtain the PMMA/ZrO_2-NC hybrid sol.

Preparation of PMMA/ZrO_2-NC hybrid films

The PMMA/ZrO_2-NC hybrid films were prepared as follows. The PMMA/ZrO_2-NC hybrid sol was cast in a PFA container and cured at 60 °C for 30 min, at 90 °C for 30 min and then at 120 °C for 1 h. Hybrid thin films ~2 μm thick were formed on a quartz glass substrate by spin coating to characterize the optical transmittance and refractive index.

We also investigated the difference between the thermal and optical properties of hybrid films and blend composite films. ZrO_2-NCs with acetate anion obtained from ZrO_2-NC aqueous sol, the MPTS-modified ZrO_2-NCs and PMMA sol (Table 1, Run 5) were mixed, stirred for 30 min and formed into blend composite films, as described above. The compositions of the blend composites are shown in Table 2. The curing process was the same as that for PMMA/ZrO_2-NC hybrid films.

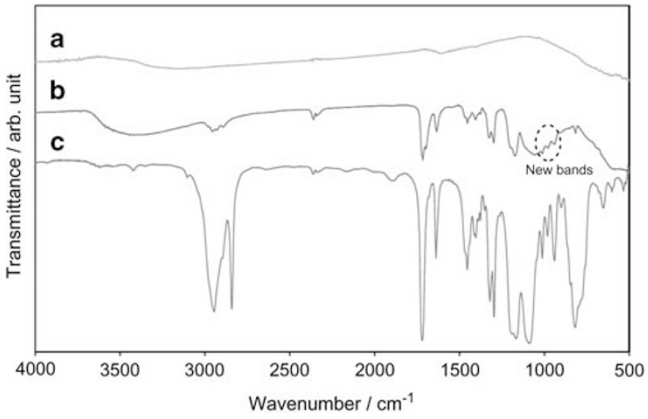

Figure 1 Fourier transform infrared (FT-IR) spectra of (a) bare zirconium oxide nanocrystals (ZrO_2-NCs), (b) 3-(methacryloxy)propyl-trimethoxysilane (MPTS)-modified ZrO_2-NCs and (c) MPTS.

RESULTS AND DISCUSSION

Characterization of MPTS-modified ZrO_2-NCs as macromonomers

FT-IR spectra of MPTS-modified ZrO_2-NCs and pure ligands are presented in Figure 1. A spectrum obtained from bare ZrO_2-NCs is shown for comparison. The major peaks that can be attributed to MPTS (Figure 1c) are the ester functionality at 1295 and 1320 cm^{-1}, the ester vibrations (C–O–C in the ester group) at 1156 and 1179 cm^{-1}, the vinyl C = C stretching mode at 1637 cm^{-1}, the carbonyl C = O stretching mode at 1716 cm^{-1} and the C-H stretching vibrations at 2840–3000 cm^{-1}. The bands at 500–850 cm^{-1} and 1050–1110 cm^{-1} are due to Zr-O and Si-O bonds, respectively. The spectrum of MPTS-modified ZrO_2-NCs (MPTS/ZrO_2 = 6.04/12.2 mmol) in Figure 1b shows bands in the range of 800–1100 cm^{-1} that arise due to the Si-O-Zr bond. This indicates the formation of a chemical bond between ZrO_2 and MPTS ligands. MPTS molecules form a chemical bond to the metal oxide surface, which is thought to progress because of the hydrolysis of one or more of the alkoxy groups, followed by condensation with surface hydroxyl groups. The band in the MPTS-modified ZrO_2-NCs spectrum occurring at 1640–1750 cm^{-1} (Figure 1b) reveals that the absorption peak associated with the carbonyl group of surface-bound MPTS splits into two peaks, one strong peak at 1713 cm^{-1} and one shoulder at 1693 cm^{-1}, corresponding to the vibration of free and associated carbonyl groups, respectively. The association of carbonyl groups is probably caused by the surface hydroxyl groups of ZrO_2-NCs or by the residual silanol groups of MPTS, namely, hydrogen-bonding interactions.

Thermogravimetric analysis was used to quantify the density of hydroxyl groups on ZrO_2-NCs (Figure 2a). According to reports in the literature,[40,41] physically adsorbed water can be removed at 120 °C, indicating that weight loss above 120 °C resulted from the removal of hydroxyl groups on the ZrO_2-NC surface. Weight loss could potentially arise from the desorption of volatile organic compounds left from particle processing; however, FT-IR spectra (Figure 1a) confirmed that there were no volatile organic compounds on the particles. A value of 9.7 OH nm^{-2} calculated using TGA weight loss and specific surface areas was obtained, which is comparable to the previously mentioned values of 10.3–10.8 OH nm^{-2} for ZrO_2.[38,41] The significant mass loss in the TGA of MPTS-modified ZrO_2-NCs (MPTS/ZrO_2 = 6.04/12.2 mmol, Figure 2b) indicated that the grafting of MPTS on treated ZrO_2 nanocrystals was successful. Quantification of the amount of grafted MPTS was calculated from TG mass losses, assuming that thermal degradation begins with methacrylic acid loss, followed by allylic radical loss. The loss of methacrylic acid above 150 °C and the loss of allylic radicals above 250 °C were confirmed, and the weight loss above 150 °C was therefore attributed to the pyrolysis of the organic component of MPTS. TGA of MPTS yielded a value of 6.82–12.1 MPTS nm^{-2} (11.3–20.1 μmol m^{-2}, Table 3), which was higher than the previously published values of 1.7–3.4 MPTS nm^{-2} (2.8–5.7 μmol m^{-2}) for ZrO_2.[38] The amount of grafted MPTS gradually increased with the amount of MPTS used during processing, as seen in Table 3. If we assume that MPTS has a molecular area of 0.60 nm^2,[42] a single coating of the silane would result in a maximum surface density of 1.7 MPTS nm^{-2} (2.8 μmol m^{-2}). As calculations indicated a much higher density, this suggests either the formation of MPTS multicoatings or the aggregation of MPTS on the surface. The excess water that exists in the reaction solution suggests that MPTS homopolymerization also took place.

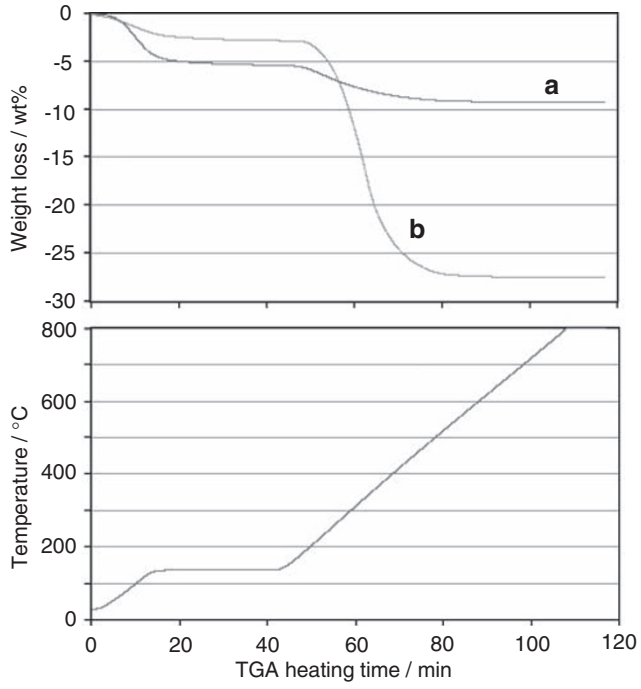

Figure 2 Thermogravimetric analysis (TGA) comparisons of (a) pure zirconium oxide nanocrystals (ZrO_2-NCs) and (b) 3-(methacryloxy)propyl-trimethoxysilane (MPTS)-modified ZrO_2-NCs (Table 1, Run 4). The diagram indicates the TGA temperature profile.

From FT-IR analysis (Figure 1), we know that the Zr-O-Si chemical bonding is the primary force holding the molecule at the surface. Hydrogen bonding through a carbonyl group has only a minor role, as indicated by FT-IR spectroscopy data (Figure 1b). The improvement in interface adhesion between ZrO_2-NC and the matrix was established by covalent bonding between the two phases. Thus, MPTS-modified ZrO_2-NCs could be used as macromonomers in grafting from the polymerization of organic monomers.

Characterization of PMMA/ZrO_2-NC hybrid sols

The PMMA/ZrO_2-NC hybrid sols were synthesized using a radical polymerization reaction of MMA monomer, MPTS-modified ZrO_2-NC as a macromonomer and 2-ethoxyethanol as a solvent. We used MPTS-modified ZrO_2 powder with 2.06 mmol g^{-1} of MPTS molecules (Table 3, M-3). The results obtained from hybrids with surface-polymerized ZrO_2-NCs are summarized in Table 1. The PMMA/ZrO_2-NC hybrid sols with a high ZrO_2-NC content had precipitates consisting of PMMA and ZrO_2-NCs aggregates (Table 1, Run 1). However, the dispersivity of ZrO_2-NCs for the sample with an MMA/MPTS molar ratio of 5:1 was clearly improved, and the material was translucent (Run 2). For the sample with an MMA/MPTS molar ratio of 10:1, the transparency of hybrid sols was considerably improved, and homogeneous PMMA/ZrO_2-NC hybrid sols were obtained (Run 3, 4). This indicates an improvement in the dispersion stability for ZrO_2-NCs in hybrid sols, most likely arising from the protective effect of PMMA polymer chains that resulted from polymerization of MMAs. A control sample of PMMA without ZrO_2 was transparent, confirming the good film-forming property of the PMMA homopolymer (Run 5).

The homogeneity of hybrid sols with PMMA was examined by TEM (Figure 3) and ultraviolet-visible transmittance (Figure 4) measurements. As shown in Figure 3a, the obtained MPTS-modified ZrO_2-NCs were easily dispersed in 2-ethoxyethanol, although unmodified

Table 3 Hydroxyl groups and grafted MPTS surface densities for ZrO_2-NCs[a]

Sample name	*Hydroxyl groups surface densities measured by TGA (OH nm^{-2})*	*MPTS surface densities*		*Dispersivity to 2-ethoxyethanol*
		Added amount (MPTS nm^{-2})	*Grafted amount measured by TGA (MPTS nm^{-2})[b]*	
M-1		7.15 (11.9 μmol m^{-2})	6.82 (11.3 μmol m^{-2})	Turbid
M-2	9.72 (16.1 μmol m^{-2})[c]	10.7 (17.8 μmol m^{-2})	9.10 (15.1 μmol m^{-2})	Transparent
M-3		14.3 (23.7 μmol m^{-2})	12.1 (20.1 μmol m^{-2})	Transparent

Abbreviations: MPTS, 3-(methacryloxy)propyl-trimethoxysilane; TGA, thermogravimetric analysis; ZrO_2-NCs, zirconium oxide nanocrystals.
[a]Specific surface area of ZrO_2-NCs was 170 $m^2 g^{-1}$ from our previous report.[37]
[b]Grafted MPTS molecule onto ZrO_2-NC was assumed as completely cross-linked silane, '$CH_2(CH_3)C(CO)OC_3H_6SiO_{1.5}$', and then forming inorganic SiO_2 after pyrolysis of organic component.
[c]Data were calculated by the weight loss of 120–800 °C of pure ZrO_2-NCs, assuming that the surface of ZrO_2-NC is free of OH surface groups at 800 °C.

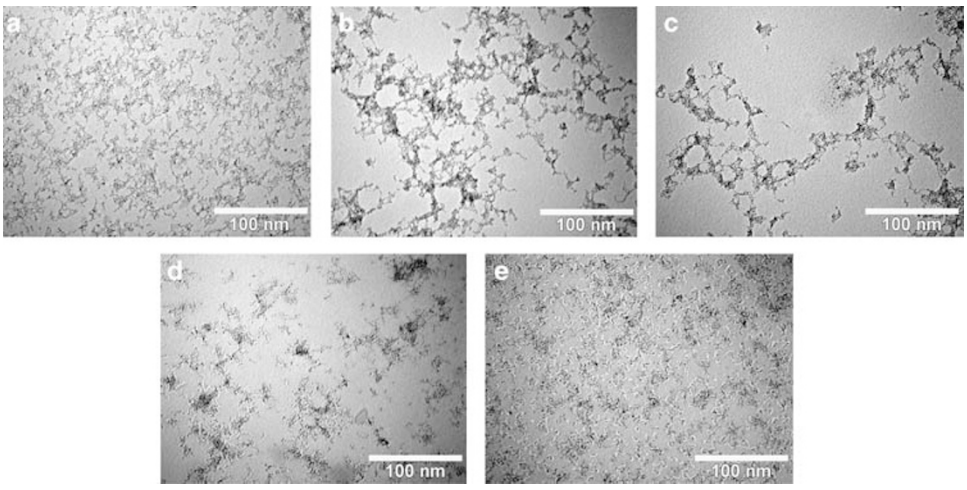

Figure 3 Transmission electron microscopy images of hybrid sols for (**a**) 3-(methacryloxy)propyl-trimethoxysilane (MPTS)-modified zirconium oxide nanocrystals (ZrO_2-NCs), (**b**) methyl methacrylate (MMA)/MPTS-ZrO_2=1/1 (Run 1), (**c**) MMA/MPTS-ZrO_2=5/1 (Run 2), (**d**) MMA/MPTS-ZrO_2=10/1 (Run 3) and (**e**) MMA/MPTS-ZrO_2=25/1 (Run 4).

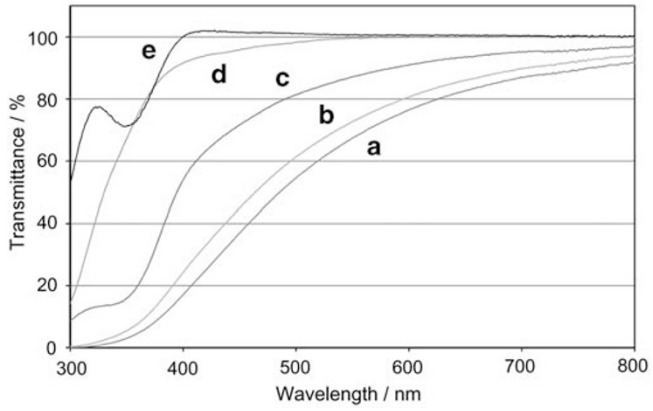

Figure 4 Optical transmittance of hybrid sols for (a) methyl methacrylate (MMA)/3-(methacryloxy)propyl-trimethoxysilane (MPTS)-zirconium oxide (ZrO_2)=5/1 (Run 2), (b) MMA/MPTS-ZrO_2=10/1 (Run 3), (c) MMA/MPTS-ZrO_2=25/1 (Run 4), (d) MPTS-modified ZrO_2 nanocrystals (ZrO_2-NCs) and (e) homopolymerized poly(methyl methacrylate) (PMMA) (Run 5). Operating light transmittance length was 10 mm.

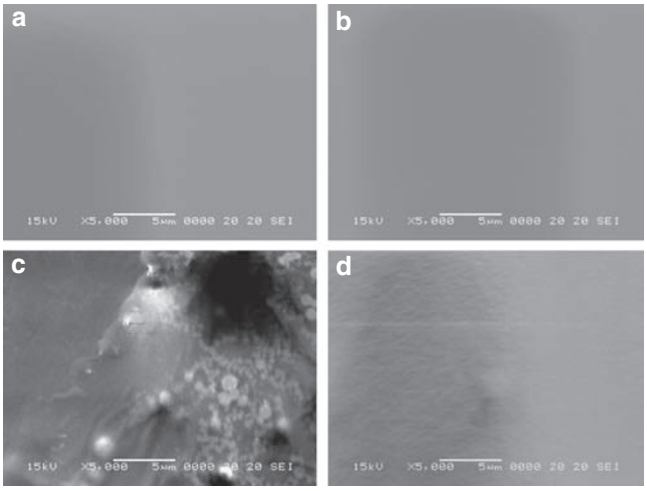

Figure 5 Scanning electron microscopy images of poly(methyl methacrylate) (PMMA)/zirconium oxide nanocrystal (ZrO_2-NC) hybrids for (**a**) a methyl methacrylate (MMA)/3-(methacryloxy)propyl-trimethoxysilane (MPTS)-ZrO_2 molar ratio of 10:1 (Run 3) and (**b**) an MMA/MPTS-ZrO_2 molar ratio of 25:1 (Run 4), and PMMA blend composite for (**c**) acetate anion-modified ZrO_2-NCs (Run 6) and (**d**) MPTS-modified ZrO_2-NCs (Run 7).

ZrO_2-NCs could not be dispersed in this medium. This result indicates that heating during the modification reaction caused MPTS molecules to attach to ZrO_2-NCs, increasing the solubility of ZrO_2-NCs in 2-ethoxyethanol. On the other hand, the sample with an MMA/MPTS molar ratio of 1:1 (Figure 3b), fabricated by the radical polymerization of MMA with MPTS-modified ZrO_2-NCs, contained aggregates resulting from nanocrystal cross-linking. These aggregates were also clearly seen in TEM images of hybrid MMA/MPTS with a molar ratio of 5:1 (Run 2, Figure 3c). However, in the translucent hybrid sol with an MMA/MPTS molar ratio of 10:1 (Run 3), homogeneity was clearly increased. A small amount of cross-linking was also observed by TEM (Figure 3d). In the hybrid sol with an MMA/MPTS molar ratio of 25:1, these assemblies disappeared (Figure 3e). This indicates that the dispersion stability for ZrO_2-NCs in hybrid sols is improved, which can be attributed to the increased protective effect of PMMA polymer chains.

The homogeneity of PMMA/ZrO_2-NC hybrid sols was examined by ultraviolet-visible transmittance (Figure 4). The translucent hybrid sols (Run 2, 3) showed low transmittance in the region of visible light because of scattering loss caused by the aggregates of cross-linked nanocrystals. Transparency was improved in the hybrid sol that had a high PMMA (Figure 4c) content, making it more suitable as an optical transparent hybrid material. Using MPTS-modified ZrO_2-NCs as macromonomers, PMMA/ZrO_2-NC hybrid sols with controlled dispersion of ZrO_2-NCs in the PMMA matrix were obtained.

Characteristic comparisons between PMMA/ZrO_2-NC hybrids and blend composites

The PMMA/ZrO_2-NC hybrid films were formed by first casting hybrid sols (Table 1, Run 1–5) and then heating them to evaporate the solvent. Blend composite films were prepared as mentioned above. The compositions of blend composites are shown in Table 2.

The dispersivity of the PMMA and ZrO_2 phases was examined by SEM (Figure 5). Phase separation of the blend composite with acetate anion-modified ZrO_2-NCs (Run 6) was observed (Figure 5c). Bright

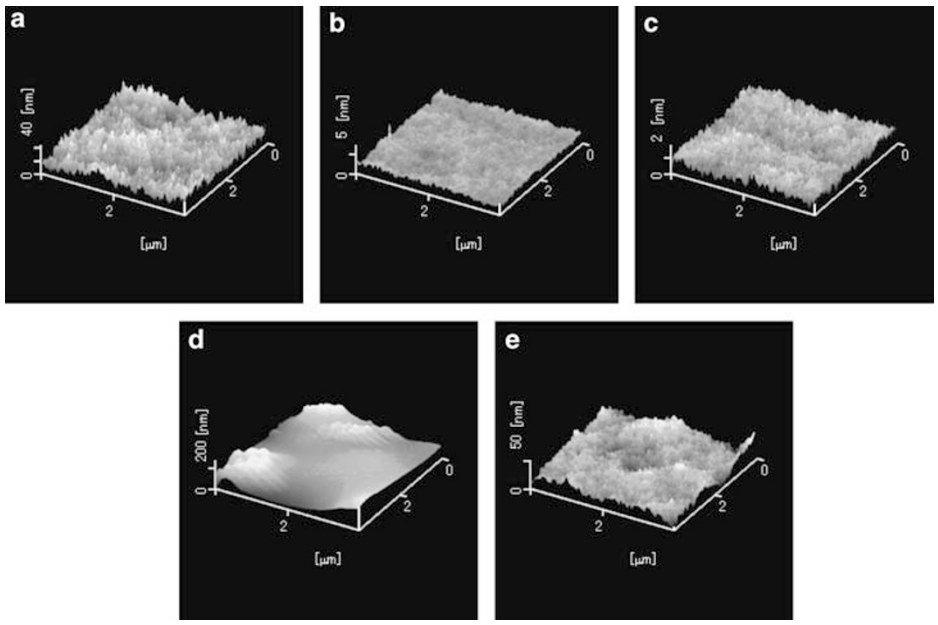

Figure 6 Tapping-mode atomic force microscopy (TM-AFM) images of (**a**) methyl methacrylate (MMA)/3-(methacryloxy)propyl-trimethoxysilane (MPTS)-zirconium oxide (ZrO_2), molar ratio of 10:1 (Run 3), (**b**) MMA/MPTS-ZrO_2, molar ratio of 25:1 (Run 4) and (**c**) poly(methyl methacrylate) (PMMA) homopolymer (Run 5), and PMMA blend composite for (**d**) acetate anion-modified ZrO_2 nanocrystals (ZrO_2-NCs) (Run 6) and (**e**) MPTS-modified ZrO_2-NCs (Run 7).

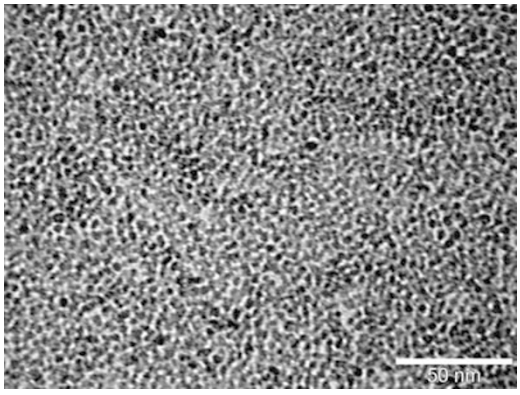

Figure 7 Transmission electron microscopy image of methyl methacrylate (MMA)/3-(methacryloxy)propyl-trimethoxysilane (MPTS)-zirconium oxide (ZrO_2), molar ratio of 10:1 (Run 3).

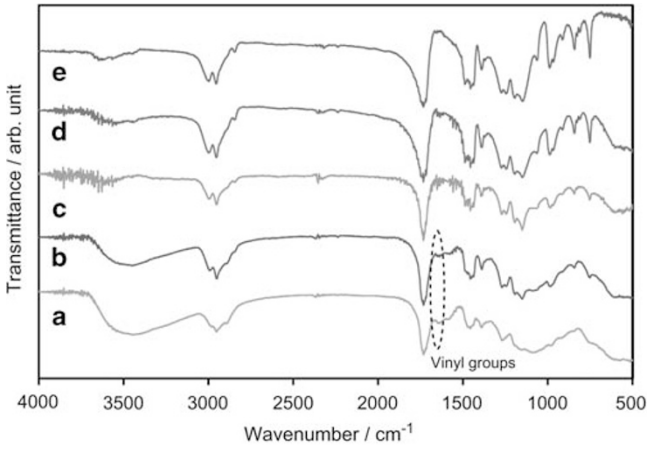

Figure 8 Fourier transform infrared (FT-IR) spectra of (a) methyl methacrylate (MMA)/3-(methacryloxy)propyl-trimethoxysilane (MPTS)-zirconium oxide (ZrO_2), molar ratio of 1:1 (Run 1), (b) MMA/MPTS-ZrO_2, molar ratio of 5:1 (Run 2), (c) MMA/MPTS-ZrO_2, molar ratio of 10:1 (Run 3), (d) MMA/MPTS-ZrO_2, molar ratio of 25:1 (Run 4) and (e) poly(methyl methacrylate) (PMMA) homopolymer (Run 5).

spots indicate ZrO_2-NC aggregates. In Figure 5d, small surface asperities confirm the slight miscibility difference between PMMA chains and MPTS-modified ZrO_2-NCs, which can be attributed to the poor chemical interaction for each component. In contrast, in the case of PMMA/ZrO_2-NC hybrids (Run 3, 4), ZrO_2-NCs are dispersed completely (Figures 5a and b). It is thus expected that ZrO_2-NCs are dispersed at the nanometer level.

The homogeneity of hybrids and blend composites was examined by TM-AFM (Figure 6). The blend composite of PMMA and acetate anion-modified ZrO_2-NCs (Run 6) showed high surface roughness (Figure 6d). In Figure 6e, the blend composite of PMMA and MPTS-modified ZrO_2-NCs (Run 7) exhibited a crenellated surface topology. On the other hand, the surfaces of PMMA/ZrO_2-NC hybrids (Figures 6a and b, Run 3, 4) and PMMA homopolymer (Figure 6c, Run 5) were extremely smooth, although surface roughness was shown to increase slightly with an increasing amount of ZrO_2-NCs. As shown in Figure 7, ZrO_2-NCs were well dispersed in the PMMA polymer matrix. TM-AFM and TEM observations further support the hypothesis that covalent bonding between PMMA and MPTS-modified ZrO_2-NC as a macromonomer is crucial to obtain nanoscale dispersed hybrid materials.

Figure 8 shows the FT-IR spectra of PMMA/ZrO_2-NC hybrids (Table 1, Run 1–5). The FT-IR spectra of MPTS-modified ZrO_2-NCs revealed the presence of numerous hydroxyl groups as indicated by the large OH stretching band, ca. 3500 cm^{-1} (Figure 1b), primarily because of physisorbed water. The intensity of this absorption band

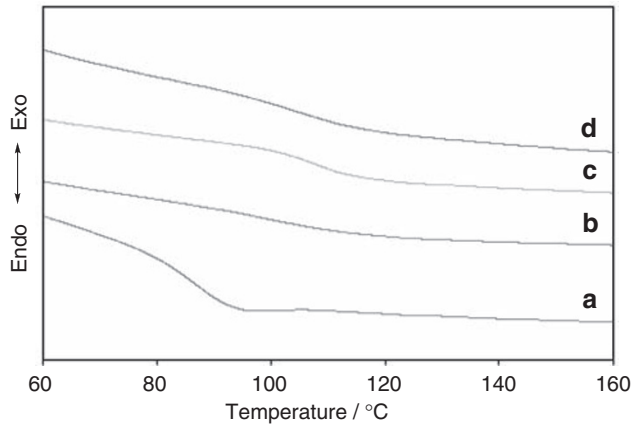

Figure 9 Differential scanning calorimetry (DSC) thermograms of (a) poly(methyl methacrylate) (PMMA) homopolymer (Run 5), (b) methyl methacrylate (MMA)/3-(methacryloxy)propyl-trimethoxysilane (MPTS)-zirconium oxide (ZrO_2), molar ratio 10:1 (Run 3) and PMMA blend composite for (c) acetate anion-modified ZrO_2 nanocrystals (ZrO_2-NCs) (Run 6) and (d) MPTS-modified ZrO_2-NCs (Run 7).

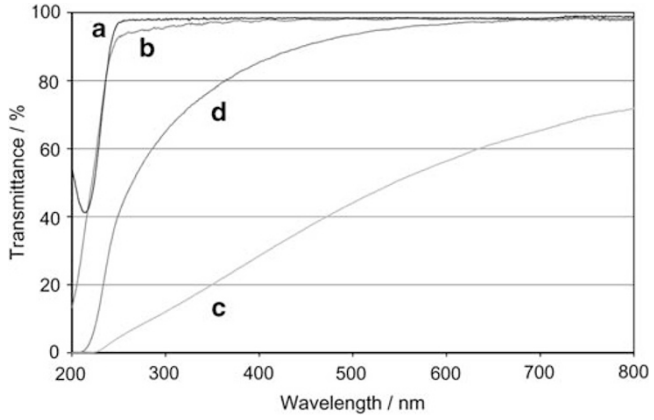

Figure 10 Thermogravimetric analysis (TGA) traces of (a) poly(methyl methacrylate) (PMMA) homopolymer (Run 5), (b) methyl methacrylate (MMA)/3-(methacryloxy)propyl-trimethoxysilane (MPTS)-zirconium oxide (ZrO_2), molar ratio of 10:1 (Run 3) and PMMA blend composite for (c) acetate anion-modified ZrO_2 nanocrystals (ZrO_2-NCs) (Run 6) and (d) MPTS-modified ZrO_2-NCs (Run 7).

gradually decreased with an increase in polymerized PMMA content, suggesting that PMMA/ZrO_2-NC hybrids harbor an increased hydrophobicity (Figured 8c and d). In the FT-IR spectra of PMMA/ZrO_2-NC hybrids, the absorption band referring to the C=C bond at 1637 cm^{-1} is also present. These bands are visible in the spectra shown in Figures 8a and b, but they are not seen in those shown in Figures 8c–e, implying the complete polymerization of MMA monomers and MPTS moieties. The incomplete polymerization of MMA and MPTS-modified ZrO_2-NCs in the samples shown in Figures 8a and b is probably the result of a low MMA monomer concentration. Further optimization of the polymerization condition (such as polymerization temperature, polymerization time, initiator concentration, and so on) is needed.

The thermal properties of hybrids and blend composites were examined by differential scanning calorimetry (Figure 9) and TGA (Figure 10). The PMMA homopolymer (Run 5) had a glass transition

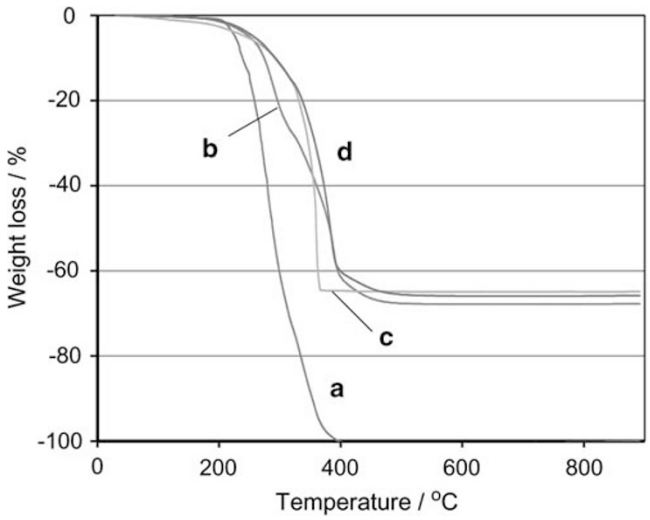

Figure 11 Optical transmittance of (a) poly(methyl methacrylate) (PMMA) homopolymer (Run 5), (b) methyl methacrylate (MMA)/3-(methacryloxy) propyl-trimethoxysilane (MPTS)-zirconium oxide (ZrO_2), molar ratio of 10:1 (Run 3) and PMMA blend composite for (c) acetate anion-modified ZrO_2 nanocrystals (ZrO_2-NCs) (Run 6) and (d) MPTS-modified ZrO_2-NCs (Run 7).

temperature (T_g) of 78.6 °C. The PMMA/ZrO_2-NC hybrid (Table 1, Run 3) and blend composites (Table 2, Run 6, 7) had a T_g that was higher than that of the PMMA homopolymer. These results indicate that ZrO_2-NCs serve as an effective inhibitor for segmental mobility of PMMA.

The thermal stabilities of hybrids and blend composites were also studied with TGA. The weight loss observed in the PMMA/ZrO_2-NCs hybrid (Figure 10b) was shifted to a higher temperature compared with that of the PMMA homopolymer (Figure 10a). This implies that ZrO_2-NCs were successfully incorporated into the hybrid material network. In general, the stage of weight loss is similar to that of the homopolymer (Table 1, Run 5), starting at ~200 °C and ending at 450 °C, which is probably because of the structural decomposition of polymers. From the curve shown in Figure 10c, the weight loss of the blend composite (Table 2, Run 6) occurred below 200 °C, which is attributed to the thermal decomposition of acetate anion. Rapid weight loss near 350 °C is attributed to the burning of organic moieties. In contrast, the PMMA- and MPTS-modified ZrO_2-NC blend composite showed high thermal stability at high temperature (Figure 10d). This could be due to the formation of stabilized organic moieties by the agglomeration of ZrO_2-NCs. Results confirm that the thermal properties of PMMA were improved by hybridization with ZrO_2-NCs.

Optical transparency of PMMA/ZrO_2-NC hybrid or blend composite films was characterized by collecting ultraviolet-visible spectra. Figure 11 shows the optical transmittance of a quartz glass substrate coated with hybrid or blend composite films. The transparency of the PMMA/ZrO_2-NC hybrid (Run 3) is similar to that of the PMMA homopolymer (Run 5), with the transmittance of the film above 95% in the visible region. The high transparency of the hybrid material in the visible region provides further evidence that ZrO_2-NCs in the PMMA matrix are nanoscale and well dispersed. On the other hand, a low optical transmittance of blend composites was observed because of the light scattering arising from phase separation of PMMA and surface-modified ZrO_2-NCs, which was also observed in SEM images (Figures 5c and d).

Table 4 Refractive indices of PMMA/ZrO_2-NC hybrids[a]

Run	*2*	*3*	*4*	*5 (PMMA)*
Refractive index (at 594 nm)	1.53407	1.52317	1.50359	1.48829

Abbreviations: PMMA, poly(methyl methacrylate); ZrO_2-NC, zirconium oxide nanocrystal.
[a]Measured by prism coupler.

The refractive indices of the transparent hybrid and PMMA homopolymer films (Run 3–5), as determined by a prism coupler, are shown in Table 4. The refractive index at 594 nm of the PMMA/ZrO_2-NC hybrid film increased from 1.488 to 1.534 when the weight content of ZrO_2-NCs was increased from 0 wt% (Run 5) to 38.8 wt% (Run 3). The increase in the ZrO_2 component results in a linear increase in the refractive index. Thus, the refractive index can be tuned by manipulating this parameter, as shown in Table 4. In this paper, we used ZrO_2 crystals with 3 nm as an inorganic component, so that a hybrid material with not only high transparency but also high refractive index could be obtained through the hybridization of PMMA- and MPTS-modified ZrO_2-NCs. These results show the excellent optical properties of PMMA/ZrO_2-NC hybrids, which is the most important characteristic when considering application in optical devices.

CONCLUSION

Transparent and homogeneous hybrid materials were prepared from PMMA- and MPTS-modified ZrO_2-NCs, which were used as macromonomers in grafting from polymerization of MMA. FT-IR confirmed that inorganic and organic moieties were covalently bonded. ZrO_2-NCs were homogeneously dispersed in polymerized hybrid sols and PMMA bulk hybrids. Hybrid films retained good optical transparency because of the formation of nanometer miscibility and good affinity between PMMA and ZrO_2-NCs compared with that of PMMA/ZrO_2-NC blend composites. Owing to their excellent optical properties and high thermal stability, PMMA/ZrO_2-NC hybrids have great potential for application in optical and mechanical fields.

1 Novak, B. M. Hybrid nanocomposite materials—between inorganic glasses and organic polymers. *Adv. Mater.* **5,** 422–433 (1993).
2 Schubert, U., Husing, N. & Lorenz, A. Hybrid inorganic-organic materials by sol-gel processing of organofunctional metal alkoxides. *Chem. Mater.* **7,** 2010–2027 (1995).
3 Wen, J. & Wilkes, G.L. Organic/inorganic hybrid network materials by the sol-gel approach. *Chem. Mater.* **8,** 1667–1681 (1996).
4 Schmid, G., Maihack, V., Lantermann, F. & Peschel, S. Ligand-stabilized metal clusters and colloids: properties and applications. *J. Chem. Soc. Dalton Trans.* 589–595 (1996).
5 Beecroft, L. L. & Ober, C. K. Nanocomposite materials for optical applications. *Chem. Mater.* **9,** 1302–1317 (1997).
6 Mucic, R. C., Storhoff, J. J., Mirkin, C. A. & Letsinger, R. L. DNA-directed synthesis of binary nanoparticle network materials. *J. Am. Chem. Soc.* **120,** 12674–12675 (1998).
7 Bohren, C. F. & Huffman, D. R. *Absorption and Scattering of Light by Small Particles* (Wiley: New York, 1983).
8 Wei, Y., Wang, W., Yeh, J. M., Wang, B., Yang, D. & Murray, J. K. Jr. Photochemical synthesis of polyacrylate-silica hybrid sol-gel materials catalyzed by photoacids. *Adv. Mater.* **6,** 372–374 (1994).
9 Wei, Y., Jin, D., Yang, C. C. & Wei, G. A fast convenient method to prepare hybrid sol-gel materials with low volume-shrinkages. *J. Sol-Gel Sci. Tech.* **7,** 191–201 (1996).
10 Wei, Y., Jin, D., Brennan, D. J., Rivera, D. N., Zhuang, Q., DiNardo, N. J. & Qiu, K. Atomic force microscopy study of organicinorganic hybrid materials. *Chem. Mater.* **10,** 769–772 (1998).
11 Wang, Q., Liu, N., Wang, X., Li, J., Zhao, X. & Wang, F. Conductive hybrids from waterborne conductive polyaniline and (3-glycidoxypropyl)trimethoxysilane. *Macromolecules* **36,** 5760–5764 (2003).
12 Matsuura, Y., Miura, S., Naito, H., Inoue, H. & Matsukawa, K. Nanostructured polysilane–titania hybrids and their application to porous titania thin films. *J. Organomet. Chem.* **685,** 230–234 (2003).
13 Chujo, Y., Ihara, E., Kure, S. & Saegusa, T. Synthesis of triethoxysilyl-terminated polyoxazolines and their cohydrolysis polymerization with tetraethoxysilane. *Macromolecules* **26,** 5681–5686 (1993).
14 Chujo, Y., Matsuki, H., Kure, S., Saegusa, T. & Yazawa, T. Control of pore-size of porous silica by means of pyrolysis of an organic-inorganic polymer hybrid. *J. Chem. Soc. Chem. Commun.* 635–636 (1994).
15 Tamaki, R., Samura, K. & Chujo, Y. Synthesis of polystyrene and silica gel polymer hybrids via ∂–∂ interactions. *Chem. Commun.* 1131–1132 (1998).
16 Tamaki, R. & Chujo, Y. Synthesis of polystyrene and silica gel polymer hybrids utilizing ionic interactions. *Chem. Mater.* **11,** 1719–1726 (1999).
17 Ogoshi, T. & Chujo, Y. Synthesis of organic–inorganic polymer hybrids utilizing amphiphilic solvent as a compatibilizer. *Bull. Chem. Soc. Jpn.* **76,** 1865–1871 (2003).
18 Ogoshi, T. & Chujo, Y. Synthesis of photosensitive organicinorganic polymer hybrids by utilizing caged photoactivatable alkoxysilane. *Macromolecules* **37,** 5916–5922 (2004).
19 Ogoshi, T. & Chujo, Y. Synthesis of organicinorganic polymer hybrids by means of hostguest interaction utilizing cyclodextrin. *Macromolecules* **36,** 654–660 (2003).
20 Ogoshi, T., Itoh, H., Kim, K. M. & Chujo, Y. Synthesis of organicinorganic polymer hybrids having interpenetrating polymer network structure by formation of ruthenium-bipyridyl complex. *Macromolecules* **35,** 334–338 (2002).
21 Ogoshi, T., Fujikawa, T., Bertolucci, M., Galli, G., Chiellini, E., Chujo, Y. & Wynne, K. J. Tapping mode AFM evidence for an amorphous reticular phase in a condensation-cured hybrid elastomer: α,ω-dihydroxypoly(dimethylsiloxane)/poly(diethoxysiloxane)/fumed silica nanoparticles. *J. Am. Chem. Soc.* **126,** 12284–12285 (2004).
22 Huang, Z. H. & Oiu, K. Y. Preparation and thermal property of poly(methyl methacrylate)/silicate hybrid materials by the in-situ sol-gel process. *Polym. Bull.* **35,** 607–613 (1995).
23 Wang, H. T., Xu, P., Zhong, W., Shen, L. & Du, Q. Transparent poly(methyl methacrylate)/silica/zirconia nanocomposites with excellent thermal stabilities. *Polym. Degrad. Stabil.* **87,** 319–327 (2005).
24 Coltrain, B. K., Landry, C. J. T., O'Reilly, J. M., Chamberlain, A. M., Rakes, G. A., Sedita, J. S., Kelts, L. W., Landry, M. R. & Long, V. K. Role of trialkoxysilane functionalization in the preparation of organic-inorganic composites. *Chem. Mater.* **5,** 1445–1455 (1993).
25 Chen, W. C. & Lee, S. J. Synthesis and characterization of poly(methyl methacrylate)-silica hybrid optical thin films. *Polym. J.* **32,** 67–72 (2000).
26 Huang, Z. H. & Qiu, K. Y. The effects of interactions on the properties of acrylic polymers/silica hybrid materials prepared by the *in situ* sol-gel process. *Polymer* **38,** 521–526 (1997).
27 Sunkara, H. B., Jethmalani, J. M. & Ford, W. T. Composite of colloidal crystals of silica in poly(methyl methacrylate). *Chem. Mater.* **6,** 362–364 (1994).
28 Jethmalani, J. M. & Ford, W. T. Diffraction of visible light by ordered monodisperse silicapoly(methyl acrylate) composite films. *Chem. Mater.* **8,** 2138–2146 (1996).
29 Joseph, R., Zhang, S. & Ford, W. T. Structure and dynamics of a colloidal silicapoly(-methyl methacrylate) composite by ^{13}C and ^{29}Si MAS NMR spectroscopy. *Macromolecules* **29,** 1305–1312 (1996).
30 Yu, Y. Y., Chen, C. Y. & Chen, W. C. Synthesis and characterization of organic–inorganic hybrid thin films from poly(acrylic) and monodispersed colloidal silica. *Polymer* **44,** 593–601 (2003).
31 Novak, B. M. & Davies, C. 'Inverse' organic-inorganic composite materials. 2. Free-radical routes into nonsbrinking sol-gel composites. *Macromolecules* **24,** 5481–5483 (1991).
32 Wei, Y., Bakthavatchalam, R. & Whitecar, C.K. Synthesis of new organic-inorganic hybrid glasses. *Chem. Mater.* **2,** 337–339 (1990).
33 Lee, L. H. & Chen, W. C. High-refractive-index thin films prepared from trialkoxysilane-capped poly(methyl methacrylate)titania materials. *Chem. Mater.* **13,** 1137–1142 (2001).
34 He, W., Guo, Z. G. & Pu, Y. K. Polymer coating on the surface of zirconia nanoparticles by inductively coupled plasma polymerization. *Appl. Phys. Lett.* **85,** 896–898 (2004).
35 Joo, J., Yu, T., Kim, Y. W., Park, H. M., Wu, F. X., Zhang, J. Z. & Hyeon, T. Multigram scale synthesis and characterization of monodisperse tetragonal zirconia nanocrystals. *J. Am. Chem. Soc.* **125,** 6553–6557 (2003).
36 Kinoshita, T. *Method for Producing Metal Oxide Nanoparticle,* JP Patent 2006-016236 (2006).
37 Otsuka, T. & Chujo, Y. Preparation and characterization of poly(vinylpyrrolidone)/zirconium oxide hybrids by using inorganic nanocrystals. *Polym. J.* **40,** 1157–1163 (2008).
38 Abboud, M., Turner, M., Duguet, E. & Fontanille, M. PMMA-based composite materials with reactive ceramic fillers Part 1.—Chemical modification and characterisation of ceramic particles. *J. Mater. Chem.* **7,** 1527–1532 (1997).
39 Turner, M., Duguet, E. & Labrugere, C. Characterization of silane-modified ZrO_2 powder surfaces. *Surf. Interface Anal.* **25,** 917–923 (1997).
40 Mueller, R., Kammler, H. K., Wegner, K. & Pratsinis, S.E. OH surface density of SiO_2 and TiO_2 by thermogravimetric analysis. *Langmuir* **19,** 160–165 (2003).
41 Wang, Z. W., Wang, T. J., Wang, Z. W. & Jin, Y. J The adsorption and reaction of a titanate coupling reagent on the surfaces of different nanoparticles in supercritical CO_2. *J. Colloid Interface Sci.* **304,** 152–159 (2006).
42 De Haan, J. W., Van Den Bogaert, H. M., Ponjee, J. J. & Van De Ven, L. J. M. Characterization of modified silica powders by fourier transform infrared spectroscopy and cross-polarization magic angle spinning NMR. *J. Colloid Interface Sci.* **100,** 591–600 (1986).